RASĀYAN *J. Chem.*
Vol. 19 | No. 4 | 2414-2423 | October-December | 2026
ISSN: 0974-1496 | e-ISSN: 0976-0083 | CODEN: RJCABP
http://www.rasayanjournal.com
http://www.rasayanjournal.co.in

METAL–DEPENDENT OPTICAL RESPONSES OF PLUMBAGIN COMPLEXES WITH Sc(III), La(III), AND Gd(III): TURN ON, UV–VIS, AND RATIOMETRIC SENSING MODES

D.T. Nhan[1], L.T.T. Tran[2], L.V. Tan[3,✉] and N.V. Thoi[4]
[1]The Dalat Nuclear Research Institute, Vietnam. Atomic Energy Institute, Vietnam
[2]Faculty of Chemistry and Environment, Dalat University, Lam Dong Province 670000, Vietnam
[3]Chemical Engineering Faculty, Industrial University of Ho Chi Minh City, 700000, Vietnam
[4]Ben Tre High School for gifted students, Vinh Long province, Vietnam.
✉Corresponding author: levantan@iuh.edu.vn

ABSTRACT
Plumbagin (5–hydroxy–2–methyl–1,4–naphthoquinone) is an oxygen-donor ligand capable of producing metal-dependent optical responses upon coordination with trivalent metal ions. This study investigates the complex formation and photophysical behavior of plumbagin with scandium, lanthanum, and gadolinium. Spectroscopic results indicate that scandium forms a complex with two ligand molecules, while lanthanum and gadolinium preferentially coordinate with three ligand molecules. The scandium system shows significant fluorescence enhancement, whereas the gadolinium system enables a ratiometric response. These findings establish plumbagin as a versatile metal–responsive chromophore, offering adaptable sensing modes for trivalent ions. Beyond fundamental coordination chemistry, this research provides a potential analytical platform for trace metal detection, which directly supports the United Nations Sustainable Development Goal (SDG) 9: Industry, Innovation, and Infrastructure. By demonstrating the structure–property relationships that govern optical signalling, this work addresses the critical challenge of selective metal ion quantification in industrial and environmental monitoring, providing a robust framework for future sensor development.
Keywords: Plumbagin, Trivalent Metal Ions, Coordination Chemistry, Photophysical Properties, Ratiometric Fluorescence Sensing, Structure–Property Relationship, Ultraviolet Visible Spectroscopy.
RASĀYAN *J. Chem.*, Vol. 19, No.4, 2026

INTRODUCTION

Plumbagin (PLB, 5–hydroxy–2–methyl–1,4–naphthoquinone) is a naphthoquinone found extensively in plants belonging to the Plumbaginaceae family. This compound has attracted considerable attention due to its diverse chemical and biological activities, including antimicrobial, anticancer, and anti–inflammatory activities. Furthermore, the presence of a conjugated quinone system and multiple oxygen donor sites allows PLB to exhibit strong metal–binding capability, forming stable complexes with a variety of metal ions.[1–3] Metal–ligand coordination involving oxygen donor ligands has been extensively investigated in coordination chemistry and analytical chemistry. When organic chromophores coordinate with metal ions, significant changes in their electronic structure may occur, resulting in alterations of optical properties such as absorption and fluorescence spectra.[4,5] These metal–induced spectral changes have been widely exploited in the development of optical probes and chemical sensors for metal ion detection.[6–9] Among various metal ions, trivalent metals such as scandium and lanthanides exhibit unique coordination chemistry due to their elevated charge density and flexible coordination numbers. Scandium(III) typically forms relatively compact complexes as a result of its smaller ionic radius, while lanthanide ions such as La(III) and Gd(III) generally possess larger ionic radii and higher coordination numbers, which allow them to bind with multiple ligand molecules.[10,11] These structural differences can significantly influence the stability and photophysical properties of metal–ligand complexes. In recent years, several studies have demonstrated that natural organic ligands can serve as effective chromophoric platforms for sensing metal ions through spectroscopic responses. In particular, coordination of metal ions with quinone or flavonoid derivatives often produces significant changes in UV–Vis absorption and fluorescence emission, which can be exploited for analytical detection.[7,12,13] Despite these advances,

http://doi.org/10.31788/RJC.2026.1949875
This work is licensed under a CC BY 4.0 license.

systematic comparative investigations of the complexation behavior of PLB across diverse trivalent metal ions remain limited. Addressing this research gap is crucial for expanding the library of natural–derived optical probes, as current literature often focuses on isolated metal–ligand interactions rather than a holistic comparative analysis. In alignment with the global objective of enhancing industrial efficiency and safety, this research directly contributes to the United Nations Sustainable Development Goal (SDG) 9: Industry, Innovation, and Infrastructure. By elucidating the structure–property relationships of PLB–metal complexes, we aim to develop cost–effective, highly selective, and innovative analytical tools that are essential for the advancement of industrial and environmental monitoring technologies. Within this study, the complexation and photophysical behavior of PLB toward three representative trivalent metal ions, Sc(III), La(III), and Gd(III), were systematically examined. By integrating UV–Vis absorption and fluorescence spectroscopy, we provide a comprehensive analysis of the stoichiometry, spectral evolution, and thermodynamic stability of these complexes. Our results reveal distinct, metal-dependent pathways-namely fluorescence enhancement for Sc(III), absorption-dominated modulation for La(III), and ratiometric fluorescence quenching for Gd(III)–which underscores the profound influence of ionic identity on the structure-property relationship of PLB. Such observations offer valuable perspectives on the structure-property relationship of PLB complexes and highlight the potential of PLB as a versatile metal-responsive chromophore for diverse analytical applications.

EXPERIMENTAL

Material and Methods

Plumbagin (PLB, 5–hydroxy–2–methyl–1,4–naphthoquinone) was procured from Sigma-Aldrich, USA. All reagents, including methanol, ethanol, DMSO, acetone, citric acid, hydrochloric acid, nitric acid, sodium hydroxide, sodium carbonate, ammonium hydroxide, and Tris.HCl, were of analytical grade and utilized without further purification. Standard solutions of scandium, lanthanum, and gadolinium ions were prepared using deionized or double-distilled water. UV–Vis absorption and fluorescence spectra were acquired with Hitachi UH5300 (Japan) and F-2700 (Japan) instruments, respectively. FT–IR analysis was conducted using a Nicolet iS50 spectrometer (USA), while thermal properties were assessed via a TGA55 instrument (USA). Structural and surface investigations involved X-ray photoelectron spectroscopy and SEM–EDS techniques. Additionally, X-ray diffraction analysis was carried out using a diffractometer (Netherlands), optical imaging was performed with a microscope (Germany), NMR spectra were obtained with a Bruker Avance Neo 600 MHz system (Switzerland), and solution pH values were monitored using a Hanna pH meter (USA).

Synthesis of PLB Metal Complexes

The synthesis of PLB metal complexes was carried out according to previously reported procedures.[5,7–9]

Spectral Studies

UV–Vis absorption spectra were recorded by mixing a fixed concentration of PLB with increasing concentrations of metal ions and recording the spectra after equilibration. For the Sc–PLB system, the PLB concentration was approximately 1.1×10^{-5} M, while for the La–PLB and Gd–PLB systems, the concentration was approximately 1.1×10^{-4} M. The spectra were recorded over an appropriate wavelength range to monitor the ligand and complex bands. Fluorescence spectra were recorded for PLB in the absence and presence of scandium, lanthanum and gadolinium ions. Emission spectra were used to evaluate fluorescence enhancement and quenching behavior. For the Gd system, measurements were carried out at pH 8.5 using an excitation wavelength of 320 nm. For the Sc system, fluorescence intensity was monitored under optimized conditions. The emission behavior was analyzed based on spectral changes and intensity variations.

Determination of Binding Parameters

For the Sc–PLB system, binding parameters were evaluated using fluorescence data based on a stepwise complexation model. The stability constants were obtained using nonlinear fitting methods. For the Gd–PLB system, fluorescence quenching behavior was examined through the Stern–Volmer approach, while binding characteristics were assessed using mole ratio and related methods. For the La–PLB and Gd–PLB

systems, stability constants were estimated from UV–Vis titration data by monitoring the evolution of complex bands.

Analytical Procedure

For Sc(III), the analytical solution was transferred into a volumetric flask, with the pH adjusted to a value of 5.5. Following the addition of the PLB solution, the mixture was diluted to the mark, and the fluorescence intensity was measured after equilibration. For Gd(III), the analytical solution was prepared at pH 8.5, followed by addition of PLB reagent. After reaction, the fluorescence intensity was monitored at 320 nm excitation, and the resulting emission signals served as the basis for analytical evaluation. Where appropriate, repeatability, recovery and comparison with reference methods were conducted following standard protocols.

RESULTS AND DISCUSSION

Comparative Complex Formation of PLB with Sc(III), La(III), and Gd(III)

PLB exhibits distinct responses toward Sc(III), La(III), and Gd(III), indicating that the identity of the trivalent ion strongly governs the coordination stoichiometry and optical output. Based on the spectral evolution and mole–ratio behavior, the Sc–PLB system is best described by a 1:2 complex, whereas both La–PLB and Gd–PLB are more consistent with 1:3 complexes. This trend is chemically reasonable because Sc(III), with its smaller ionic radius and more compact coordination sphere, typically accommodates fewer bulky bidentate ligands than the larger lanthanide ions. By contrast, La(III) and Gd(III) generally favor higher coordination numbers and show strong affinity for oxygen–donor ligands, making a 1:3 PLB stoichiometry plausible. This interpretation is also in line with earlier lanthanide–plumbagin chemistry, where La(III) and Gd(III) plumbagin complexes of the type *[Ln(PLB)$_3$]* were isolated and characterized, supporting a tris–ligand coordination pattern for lanthanides with deprotonated plumbagin–type ligands.[4–7] The comparative stoichiometric parameters and stability constants are summarized in Table-1. The corresponding UV–Vis absorption spectra of PLB and its complexes with Sc(III), La(III), and Gd(III) are shown in Fig.-1.

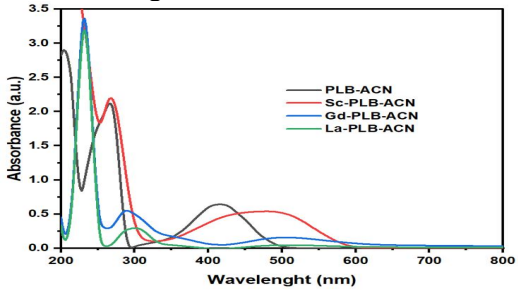


Fig.-1: Comparative UV–Vis Spectra of PLB with Sc(III), La(III), and Gd(III). UV–Vis Absorption Spectra of PLB and the Corresponding Metal–PLB complexes (Sc–PLB, Gd–PLB, and La–PLB) Recorded in Acetonitrile (ACN). $C_{PLB} = 1.0 \times 10^{-3}$ M. $C_{Sc} = 12.1 \times 10^{-4}$ M. $C_{Gd} = 2.54 \times 10^{-4}$ M. $C_{La} = 2.54 \times 10^{-4}$ M

For the present comparative paper, this stoichiometric divergence is not merely a structural detail; it is the first key that explains why the three systems do not produce the same spectral behavior. The smaller Sc(III) ion appears to promote a more compact chelate environment that strongly rigidifies the ligand and favors fluorescence turn–on. In contrast, the larger La(III) and Gd(III) ions enable a higher ligand loading, which increases cumulative complex stability but does not necessarily maximise fluorescence intensity. Thus, the present dataset already suggests an important principle: thermodynamic stability and photophysical response do not scale in parallel. This distinction becomes clearer in the UV–Vis and fluorescence sections below.

UV–Vis Spectral Evolution: Different Metals, Different Electronic Perturbations

The UV–Vis results show that all three ions perturb the electronic structure of PLB, but they do so in different ways.

Sc–PLB: Pronounced Bathochromic Shift and Visible–Band Formation

For Sc(III), free PLB shows a visible absorption band near 418 nm, while the complexed form develops a

new broad band in the visible region. The energy shift is significant, indicating that coordination lowers the energy of the dominant electronic transition, consistent with a strong perturbation of the conjugated quinone chromophore. Detailed energetic parameters corresponding to this transition are summarized in Table-1. The behaviour of Sc–PLB is also notable because the new band appears in the visible region, where PLB itself is already optically active. This makes the Sc system visually and spectroscopically attractive for sensing. Relative to previously reported PLB–Ti behaviour, where a 1:2 $Ti(PLB)_2$ complex also gives a visible–region response and strong fluorescence around 605 nm, the Sc–PLB pattern appears mechanistically related: both small, hard, oxophilic ions generate compact O, O–chelated PLB complexes associated with low–energy optical transitions. The similarity does not imply identity, but it reinforces the idea that hard, high–charge–density ions can convert PLB into a more strongly emissive, red–shifted chromophore.

La–PLB: Spectral Redistribution toward the UV Region

In contrast, the La system behaves very differently. The visible PLB band is suppressed, and a new strong band appears in the UV region. The principal spectral shift is strongly hypsochromic, with the molar absorptivity and specific wavelength detailed in Table-1. This UV–dominant behaviour suggests that La(III) coordination perturbs the ground–state electron distribution of PLB without strongly stabilising an emissive low–energy excited state. The result is a clear absorption signature but little fluorescence activation. This interpretation is chemically reasonable for a diamagnetic lanthanide ion with a $4f^0$ configuration, whose direct participation in low–lying ligand–centred radiative transitions is limited. It is also consistent with the literature precedent that La(III) readily forms oxygen–donor plumbagin complexes, but such coordination does not inherently guarantee strong ligand fluorescence.

Table-1: UV-Vis-Derived Spectroscopic and Stability Parameters of PLB Complexes with Sc(III), La(III) and Gd(III)

Complex system	Stoichiometry	λmax of free PLB (nm)	λmax of complex band(s) (nm)	Δλ(nm)	ε(L/mol/cm)	Stability constant β	logβ	ΔG^0 (kJ/mol)
Sc–PLB	1:2	~410–418	~495–500	+80 to +90	–	$\beta_2 = 5.05 \times 10^6\ M^{-2}$	6.70	–38.2
La–PLB	1:3	~420–425	~300	–120 to –125	$\varepsilon_{300} \approx 7.9 \times 10^3$	$\beta_3 \approx 8.7 \times 10^{11}\ M^{-3}$ *(apparent)*	11.94	–68.1
Gd–PLB	1:3	~420–423	~295–300; ~500–506	–125 to –128; +77 to +83*	$\varepsilon_{300} \approx 1.42 \times 10^4$; $\varepsilon_{500} \approx 4.8–4.9 \times 10^3$	$\beta_3 \approx 10^{11}$ to $7.8 \times 10^{11}\ M^{-3}$ *(apparent)*	~11.0 to 11.89	–62.8 to –63.0

* For Gd–PLB, the negative Δλ refers to the shift from the main PLB visible band (~423 nm) to the new UV band (~295–300 nm), whereas the positive value reflects the emergence of the new visible band near 500–506 nm.

Gd–PLB: Dual–Band Behaviour and the Richest UV–Vis Signature

The Gd system is the most informative from a mechanistic viewpoint. The original PLB band is strongly depleted, while two new bands emerge. The molar absorptivities and specific wavelengths are presented in Table-1. This dual–band pattern is especially important because it implies that Gd(III) does not simply "shift" the PLB spectrum; instead, it reorganises it, producing both a UV–dominant band and a visible–region band. The appearance of both bands is consistent with a mixed electronic picture: the ~300 nm band is reasonably assigned to ligand–centred or intraligand charge redistribution enhanced by coordination, whereas the new visible band suggests stronger perturbation of the PLB π–system and may include a charge–transfer contribution. A similar logic has been invoked in PLB–based metal complexes and in broader lanthanide coordination chemistry, where oxygen–donor ligation often redistributes ligand–centred transitions while also modifying low–energy excited states. The fact that Gd–PLB shows the richest UV–Vis signature, rather than the largest fluorescence enhancement, already hints that its dominant photophysical pathway differs from that of Sc–PLB. The main UV–Vis–derived parameters of

the three PLB complexes are summarized in Table-1. The results show that Sc(III) produces the most pronounced bathochromic shift, whereas La(III) and Gd(III) mainly induce strong UV–region bands associated with 1:3 complex formation. The cumulative stability constants further indicate that the lanthanide complexes are thermodynamically more stable overall than the Sc(III) complex, although this trend does not directly correlate with fluorescence enhancement. Detailed spectroscopic and stability parameters are presented in Table-1, and the interpretive notes regarding their calculation are provided in the table footnotes.

UV–Vis Comparison and Chemical Meaning

From a comparative viewpoint, the UV–Vis results establish three distinct regimes, which are summarized in Table-1:

Sc–PLB: Visible–band generation with the strongest bathochromic shift.

La–PLB: Dominant UV–band formation with little visible enhancement.

Gd–PLB: Dual–band redistribution with both UV and visible signatures.

This pattern is chemically meaningful. It indicates that coordination geometry and ionic identity do not merely affect stability; they redefine the electronic landscape of PLB in different ways. Sc(III) appears to favour a strongly conjugation–perturbing, lower–energy chromophore. La(III) stabilises a UV–dominant coordinated state. Gd(III) creates a more electronically heterogeneous complex, and this heterogeneity is echoed again in fluorescence, where the two emission channels respond differently.

Fluorescence Behaviour: Turn–On, Silent, and Ratiometric Quenching

If the UV–Vis section shows how the ground–state electronic structure changes, the fluorescence section reveals how those changes are translated–or not translated–into emissive behaviour.

Sc–PLB: Strongest Turn–On Fluorescence

The Sc system gives by far the largest fluorescence response (Fig.-2). Free PLB is nearly non–emissive, whereas the Sc–PLB complex exhibits a strong fluorescence turn–on effect. The calculated fluorescence enhancement factor (EF) is presented in Table-2, confirming the effectiveness of this system for turn-on sensing. This is a classic CHEF–like outcome: coordination suppresses non–radiative deactivation channels by rigidifying the ligand and restricting structural relaxation in the excited state. The striking contrast between the weakly emissive PLB and the highly emissive Sc–PLB complex strongly supports this rigidification–assisted mechanism.

La–PLB: Spectroscopically Evident, Photophysically Quiet

The La system is fundamentally different. Although UV–Vis clearly shows complex formation, the fluorescence spectra remain nearly superimposed. Specific emission changes are summarised in Table-2.

This "silent" behaviour is actually informative. It shows that complex formation alone is not sufficient to generate useful fluorescence output. The complex may be thermodynamically stable and spectroscopically distinct in absorption, yet the excited state of PLB may still relax in essentially the same way as the free ligand. In other words, La(III) changes the electronic distribution enough to alter the absorption spectrum, but not enough to convert PLB into an efficient fluorophore. This directly supports the broader conclusion of the paper: stability, spectral change, and fluorescence efficiency are related but non–equivalent properties.

Gd–PLB: Selective Quenching and Built–in Ratiometric Behaviour

The Gd system is the most analytically versatile. PLB shows two emissive regions, and Gd(III) quenches both–but unequally. The specific quenching percentages at 530 nm and 610 nm, along with the calculated ratiometric shifts and calibration statistics (R^2), are detailed in Table-2. This unequal suppression makes the system ratiometric, which is a highly favourable analytical situation. Ratiometric fluorescence is generally more robust than single–intensity sensing, as the ratio becomes a self–referenced signal. Mechanistically, this is chemically sensible; as a paramagnetic $4f^7$ ion, Gd(III) is known to promote nonradiative decay, which supports our assignment of differential quenching rather than fluorescence turn–on.

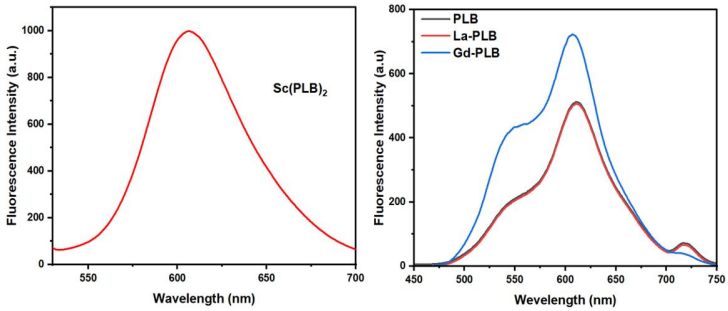


Fig.-2: Comparative Fluorescence Spectra of Sc–PLB, La–PLB and Gd–PLB

The Sc–PLB complex shows a strong fluorescence turn–on effect around 610 nm, whereas La–PLB exhibits minimal fluorescence change. In contrast, Gd–PLB produces unequal quenching of the emission bands at 530 and 610 nm, enabling ratiometric fluorescence sensing. The fluorescence characteristics of the three systems are summarised in Table-2. Among them, the Sc–PLB complex exhibits the strongest fluorescence activation, while the La–PLB system remains nearly spectroscopically silent. In contrast, Gd–PLB induces wavelength–dependent quenching, enabling a ratiometric sensing strategy based on the I_{610}/I_{530} emission ratio.

Table-2: Fluorescence Parameters of PLB complexes (EF, Q530, Q610, Ratio shift, Quenching behavior)

System	λem (nm)	Fluorescence intensity change	EF/ quenching	Ratio change	Quenching behavior	Analytical mode
PLB	530/610	reference	–	1.03	–	–
Sc–PLB	~610	30→1700 a.u.	EF ≈ 60	–	not quenching	turn–on fluorescence
La–PLB	~530/610	negligible	EF ≈ 1	~1.03	none	UV–Vis sensing
Gd–PLB	530/610	800→560 (530 nm)	Q530 ≈ 30%	1.03 → 1.29	strong quenching	ratiometric sensing
		800→720 (610 nm)	Q610 ≈ 10%	–	weaker quenching	reference channel

Stability and Thermodynamic Interpretation: why the Brightest Complex is not the Most Stable One

One of the most important conclusions of this work is that the most emissive complex is not the most thermodynamically stable one.

For Sc–PLB, the stepwise binding analysis already available from the optimised stepwise fitting gives:

$$K_1 = 1.65 \times 10^3\ M^{-1},\ K_2 = 3.06 \times 10^3\ M^{-1}$$

which leads to:

$$\beta_2 = 5.05 \times 10^6\ M^{-2},\ \log\beta_2 = 6.70$$

For La–PLB and Gd–PLB, the comparative treatment supports apparent cumulative values on the order of 10^{11}, with representative values of:

$$\beta_3 \approx 8.7 \times 10^{11}\ M^{-3},\ \log\beta_3 \approx 11.94$$

$$\beta_3 \approx 10^{11}–7.8 \times 10^{11}\ M^{-3},\ \log\beta_3 \approx 11–11.89$$

and ΔG^{o} values around –68 kJ/mol for La and –63 kJ/mol for Gd.

Even allowing for the approximate nature of the La/Gd values, the cumulative trend is clear: the 1:3 lanthanide systems are thermodynamically more stable overall than the 1:2 scandium system. That does not contradict the fluorescence data. Instead, it shows that cumulative chelate stability and excited–state radiative efficiency are controlled by overlapping but distinct factors. La and Gd gain stability from higher ligand loading and lanthanide coordination chemistry, but only Sc converts PLB into a strongly emissive complex. This is precisely the type of structure–property decoupling that makes comparative studies valuable. A more balanced comparison can be made using the average apparent affinity per

binding event, lanthanide preference for hard oxygen–donor environments and their higher coordination capacity. However, that greater affinity does not translate into CHEF. Instead, it yields either a UV–dominant response (La) or a quenching/ratiometric response (Gd). Thus, the present data support a second key principle of the paper: complex stability determines whether a complex exists strongly enough to be observed, but the metal's electronic nature determines what kind of optical signal that complex produces.

La versus Gd: Lanthanide Contraction and why Two 1:3 Complexes Behave differently

Although La(III) and Gd(III) both form 1:3 complexes with PLB, they are not spectroscopically equivalent. This difference is best understood through the combined effects of lanthanide contraction and electronic configuration. Across the lanthanide series, ionic radii decrease gradually with increasing atomic number. Reviews and structural surveys show that this contraction influences bond distances, donor preferences, and coordination–shell geometry in lanthanide complexes. In simple terms, Gd(III) is smaller and has higher effective charge density than La(III), even though both remain hard Lewis acids with a strong preference for oxygen donors. This helps explain why Gd–PLB can be at least as stable as La–PLB and, more importantly, why it perturbs the PLB chromophore more strongly in both UV–Vis and fluorescence. But lanthanide contraction alone is not enough. The decisive fluorescence difference comes from the electronic configuration. La(III) is $4f^0$ and diamagnetic, whereas Gd(III) is $4f^7$ and strongly paramagnetic. That difference is entirely consistent with the present results: La gives almost no emission change, while Gd selectively quenches PLB fluorescence and produces a ratiometric signal. In other words, La and Gd may be structurally similar as 1:3 PLB complexes, but they are photophysically different because only Gd introduces a strong paramagnetic deactivation pathway. This comparison is important because it prevents an oversimplified interpretation. It would be incorrect to say "La and Gd behave differently because one is more stable." La and Gd behave differently because one is essentially a diamagnetic lanthanide hard acid, whereas the other is a paramagnetic lanthanide hard acid of smaller radius. Both form stable PLB chelates, but only Gd is expected to impose strong excited–state quenching.

Structure–Property Relationship and Analytical Perspectives of PLB Complexes

The comparative spectroscopic and chromatographic results reveal a clear relationship between the coordination structure of PLB complexes and their preferred analytical detection modes. The three metal ions investigated–Sc(III), La(III), and Gd(III)–induce distinct electronic perturbations in the PLB chromophore, which in turn govern the optimal analytical strategy for each system.

Sc–PLB: Fluorescence turn-on Sensing

For Sc(III), the formation of the 1:2 Sc $(PLB)_2$ complex produces a pronounced bathochromic shift and strong fluorescence enhancement. The compact coordination environment created by the small Sc(III) ion rigidifies the PLB ligand and suppresses non-radiative decay pathways, resulting in a strong chelation-enhanced fluorescence (CHEF) effect. Consequently, the fluorescence intensity increases dramatically compared with free PLB. This strong fluorescence activation makes the Sc–PLB system highly suitable for direct fluorescence-based determination of Sc(III). The analytical mechanism relies on fluorescence amplification rather than quenching, which generally provides high sensitivity and low detection limits. Therefore, the structural characteristics of the Sc complex–namely the compact 1:2 chelate geometry and strong ligand rigidification–directly explain its effectiveness as a fluorescence probe (Fig.-3).

Gd–PLB: Ratiometric fluorescence sensing

In contrast, the $Gd(PLB)_3$ complex displays a fundamentally different photophysical profile. The paramagnetic property associated with the Gd(III) centre facilitates non-radiative relaxation pathways, leading to the selective inhibition of PLB fluorescence emission. Importantly, the quenching efficiency varies between the two emission wavelengths (~530 nm and ~610 nm). This unequal suppression generates a ratiometric fluorescence signal, in which the intensity ratio changes systematically with Gd(III) concentration. The I_{610}/I_{530} ratiometric signal is particularly advantageous because the ratio signal is less sensitive to experimental fluctuations, such as probe concentration, excitation intensity, or optical path length. The Gd–PLB system therefore represents an example where paramagnetic quenching becomes analytically beneficial, enabling a self-referenced fluorescence sensing strategy.

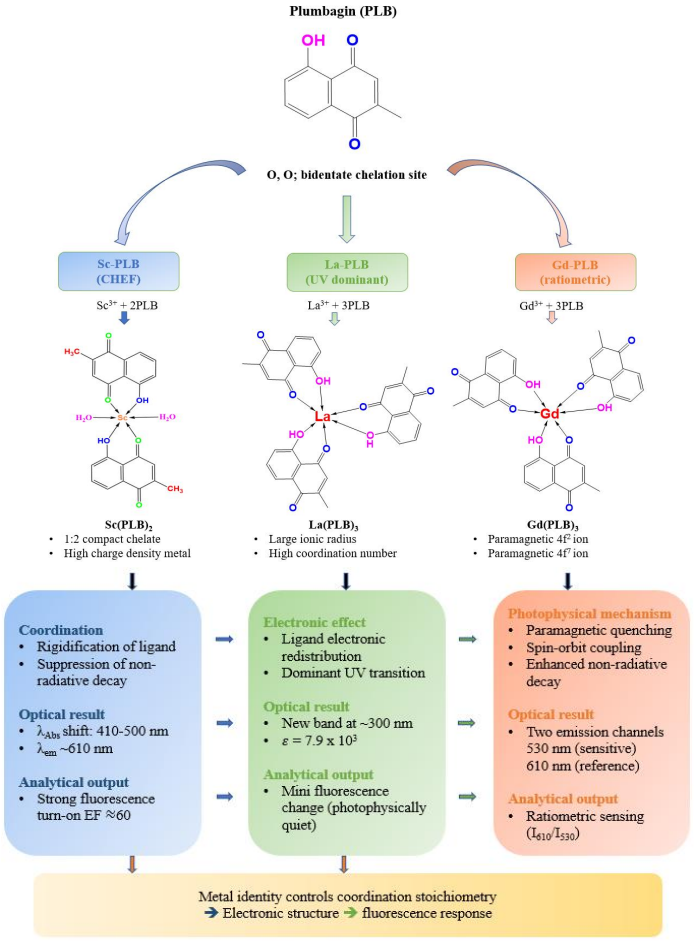


Fig.-3. Unified mechanism scheme for Sc–PLB, La–PLB, and Gd–PLB

La–PLB: Spectral Response without Fluorescence Activation

The La(PLB)$_3$ complex, despite having a similar stoichiometry to the Gd complex, does not produce significant fluorescence enhancement or quenching. Instead, the main spectral effect of La(III) coordination is the formation of a strong absorption band in the UV region (~300 nm). The diamagnetic nature of La(III) and its larger ionic radius lead to weaker perturbation of the emissive excited state of PLB. As a result, the La–PLB system is not optimal for fluorescence sensing but remains clearly detectable by absorption-based spectroscopic techniques, particularly UV–Vis spectrophotometry.

HPLC Separation Behaviour and Analytical Implications

The chromatographic results provide further insight into the analytical potential of these systems. As shown in the HPLC chromatograms (Fig.-4), free PLB and its metal complexes exhibit distinct retention behaviours. In the La–PLB system, a new peak corresponding to the complex appears at a retention time of approximately 7–8 min, clearly separated from the free ligand peak. This indicates that complex formation significantly modifies the polarity and interaction of PLB with the stationary phase. In the comparative chromatogram containing PLB, La–PLB, and Gd–PLB, three distinct signals are observed, confirming that the complexes possess sufficiently different physicochemical properties to allow chromatographic discrimination. Such separation behaviour suggests that HPLC coupled with UV detection could provide an effective strategy for the determination of La(III) through the formation of the La–PLB complex. Unlike fluorescence detection, which is not strongly responsive in the La system, chromatographic detection benefits from the pronounced absorption of the complex in the UV region. The formation of a stable La–PLB species with a distinct retention time therefore offers a promising basis for HPLC-UV analytical methods for lanthanum determination.

Integrated Analytical Perspective

Collectively, these findings indicate that the analytical utility of PLB complexes is heavily influenced by the electronic and coordination properties of the metal ion. Sc(III) forms a compact chelate that strongly enhances fluorescence, making it suitable for turn-on fluorescence detection. Gd(III) produces differential fluorescence quenching, enabling ratiometric fluorescence sensing. La(III) primarily alters the absorption spectrum and chromatographic behaviour of PLB, suggesting its suitability for UV–Vis or HPLC–UV analysis rather than fluorescence methods. The optical behaviour and preferred analytical sensing modes of the three complexes are summarized in Table-3.

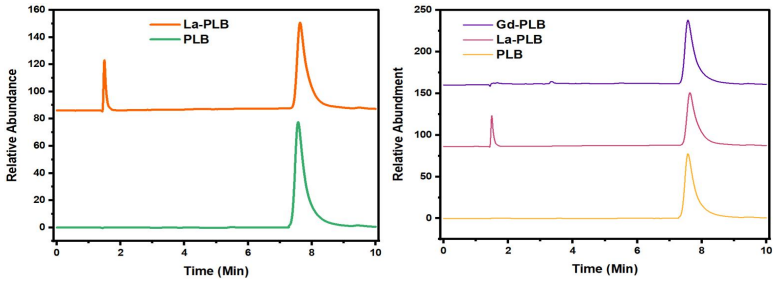


Fig.-4: HPLC Chromatograms of PLB and its Complexes with La(III) and Gd(III)

This structure–property relationship highlights the versatility of PLB as a multifunctional ligand for metal-ion detection. By selecting the appropriate detection technique according to the photophysical response of the complex, PLB-based systems can potentially serve as adaptable analytical platforms for different rare-earth and transition metal ions.

Table-3: Comparative Summary of The Optical Behaviour and Analytical Relevance of PLB Complexes

Complex system	Δλ(nm)	logβ	Fluorescence effect	Quantitative fluorescence metric	Preferred sensing mode
Sc–PLB	+85 to +90	6.70	Strong enhancement	*EF* ≈ *58-60*	Turn–on fluorescence.
La–PLB	–120 to –125	11.94	Minimal change	$I/I_0 \approx 1$	UV–Vis
Gd–PLB	–125 to –128; +77 to +83	~11.0 to 11.89	Unequal quenching	$Q_{530} \approx 30\%$, $Q_{610} \approx 10\%$, $\Delta R/R_0 \approx 25\%$	Ratiometric fluorescence

CONCLUSION

The present study demonstrates that plumbagin (PLB) exhibits distinct, metal-dependent complexation and optical responses toward Sc(III), La(III), and Gd(III). Spectroscopic analysis confirmed the formation of 1:2 Sc–PLB and 1:3 La–PLB/Gd–PLB complexes. The Sc–PLB system facilitates a bathochromic shift (~410 to ~500 nm) coupled with strong fluorescence enhancement (EF ≈ 58), consistent with a chelation-enhanced fluorescence (CHEF) effect. Conversely, La–PLB primarily generates a new UV absorption band (~300 nm) with minimal emission change, whereas Gd–PLB exhibits dual-band absorption and selective fluorescence quenching, enabling a ratiometric response. These results reveal that thermodynamic stability and photophysical performance are controlled by distinct factors, including ionic radius, coordination geometry, and electronic configuration. From an analytical perspective, this research establishes Sc–PLB as an optimal platform for turn-on fluorescence sensing, Gd–PLB for ratiometric detection, and La–PLB for UV–Vis or HPLC–based determination. Ultimately, this work highlights PLB as a versatile chromophore for trace metal analysis, with its sensing capabilities directly contributing to SDG 9: Industry, Innovation, and Infrastructure. Future research should prioritise the validation of these sensing platforms in complex, real-world industrial matrices.

ACKNOWLEDGMENTS

The authors sincerely appreciate the support from Dalat Nuclear Research Institute, CASE Service and Analysis Centre in Ho Chi Minh City, Chemical Engineering Faculty, Ho Chi Minh City University of Industry and Da Lat University for their provision of experimental conditions and essential research materials, which were instrumental in the successful completion of this study.

CONFLICT OF INTERESTS

The authors declare that there is no conflict of interest.

AUTHOR CONTRIBUTIONS

The present work is related to *SDG-9: Industry, Innovation, and Infrastructure*. All the authors contributed significantly to this manuscript, participated in reviewing/editing and approved the final draft for publication. The research profile of the authors can be verified from their ORCID ids, given below:

L.V. Tan https://orcid.org/0000-0002-1935-2183
L.T.T. Tran https://orcid.org/0000-0001-6607-2590
D.T. Nhan https://orcid.org/0009-0001-7233-1859
N.V. Thoi https://orcid.org/0009-0005-0640-2291

Open Access: This article is distributed under the terms of the Creative Commons Attribution 4.0 International License (http://creativecommons.org/licenses/by/4.0/), which permits unrestricted use, distribution, and reproduction in any medium, provided you give appropriate credit to the original author(s) and the source, provide a link to the Creative Commons license, and indicate if changes were made.
Cite this article as: D. T. Nhan *et al.*, *Rasayan J. Chem.*, 19(4), 2414-2423(2026), https://doi.org/10.31788/RJC.2026.1949875

REFERENCES

1. R. Joshi and R. Gangabhagirathi, *Journal of Radioanalytical and Nuclear Chemistry*, **303**, 919(2015), https://doi.org/10.1007/s10967-014-3501-7
2. H.H. Guan, Y.H. Huang, E.S. Lin, C.J. Chen, and C.Y. Huang, *International Journal of Molecular Sciences*, **22**, 6861(2021), https://doi.org/10.3390/ijms22136861
3. S. Liyanaarachchi, C. Padumadasa, G. Priyadarshana, F.C. Robles Hernandez, A. Dilhari, O. Sahin, S. Lakshika, G. Wijesinghe, M. Weerasekera, V. Karunaratne, Z. Wang, A. Meiyazhagan, N. Kottegoda, and P.M. Ajayan, *ACS Sustainable Chemistry & Engineering*, **9**, 1361(2021), https://doi.org/10.1021/acssuschemeng.0c08194
4. S.D. Shahida Parveen, A. Affrose, and K. Pitchumani, *Sensors and Actuators B: Chemical*, **221**, 521(2015), https://doi.org/10.1016/j.snb.2015.06.149
5. M. Tan, Y. Liu, X. Luo, Z. Chen, and H. Liang, *Bioinorganic Chemistry and Applications*, **2011**, 898726(2011), https://doi.org/10.1155/2011/898726
6. A.C.M. Dangalla and O.A. Ileperuma, *Journal of the National Science Council of Sri Lanka*, **13**, 141(1985).
7. Z.F. Chen, M.X. Tan, Y.C. Liu, Y. Peng, H.H. Wang, H.G. Liu, and H. Liang, *Journal of Inorganic Biochemistry*, **105**, 426(2011), https://doi.org/10.1016/j.jinorgbio.2010.12.003
8. D.T. Nhan, L. Van Tan, L.T.T. Tran, T.T.T. Huong, L.T. Tho, and P. Van Tat, *Microchemical Journal*, **214**, 113914(2025), https://doi.org/10.1016/j.microc.2025.113914
9. N. Van Thoi, T.N.M. An, N.Q. Hung, P. Van Tat, and L. Van Tan, *Microchemical Journal*, **194**, 109221(2023), https://doi.org/10.1016/j.microc.2023.109221
10. X. Chen, L. Yin, L. Peng, Y. Liang, H. Lv, and T. Ma, *Infection and Drug Resistance*, **13**, 2751(2020), https://doi.org/10.2147/IDR.S265753
11. Y.H. Huang, Y. Lien, J.H. Chen, E.S. Lin, and C.Y. Huang, *Biochimie*, **171–172**, 124(2020), https://doi.org/10.1016/j.biochi.2020.03.005
12. N.S. Chundawat, S. Jadoun, P. Zarrintaj, and N.P.S. Chauhan, *Polyhedron*, **210**, 115387(2021), https://doi.org/10.1016/j.poly.2021.115387
13. C. Grüttner, S. Rudershausen, S.E. Matthews, P. Wang, V. Böhmer, and J.F. Dozol, *European Cells and Materials*, **3**, 48(2002).

[RJC-9875/2026]